ACS OMEGA

http://pubs.acs.org/journal/acsodf

Article

Effect of Liquid Nitrogen Freeze–Thaw Cycles on Pore Structure Development and Mechanical Properties of Coal

Bo Li,* Zhen Shi, Zeqi Wang, and Laisheng Huang

Cite This: *ACS Omega* 2022, 7, 5206–5216

Read Online

ACCESS | Metrics & More | Article Recommendations

ABSTRACT: To improve the mining efficiency of coalbed methane, liquid nitrogen freeze–thawing experiments were performed to improve coal seam permeability and to study its influence on coal pore structure development and mechanical properties. Mechanical properties and nuclear magnetic resonance tests of coal samples were performed with 0, 5, 10, and 15 freeze–thaw cycles of liquid nitrogen. The results show that the number of freeze–thaw cycles caused the change of uniaxial compressive strength and elastic modulus of coal, and the change effect decreased significantly after 11–15 freeze–thaw cycles. Between 0 and 5 freeze–thaw cycles, the base growth rate of the transverse relaxation time T_2 spectral area of the full pore of coal is 44.1%, and that of the transverse relaxation time T_2 spectral area of adsorption pore is 71.5%. After 6–10 freeze–thaw cycles, the fixed base growth rate of the transverse relaxation time T_2 spectral area of the full hole of coal is 269.0%, and the chain growth rate is 156.2%. In this stage, the chain growth rate of the transverse relaxation time T_2 spectral area of the seepage hole is 198.4%, which is mainly the growth of seepage hole volume. After 11–15 freeze–thaw cycles, the chain growth rate of the full pore of coal transverse relaxation time T_2 spectrum area is 20.1%, the chain growth rate of adsorption pore is 4.8%, the chain growth rate of seepage pore is 22.2%, and the growth rate of the pore volume is greatly reduced. Comparing the changes of pore and coal mechanical properties in different pore sizes, it can be seen that the change of adsorption pore volume has a greater impact on coal mechanical properties.

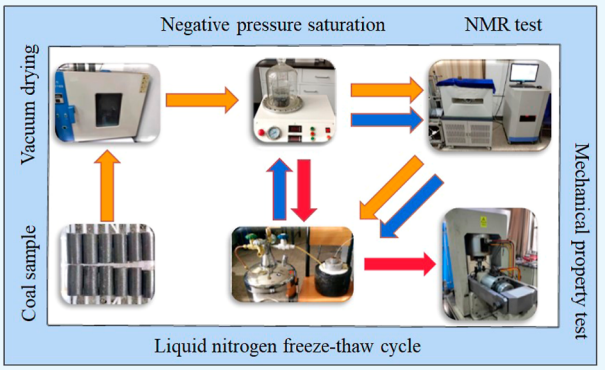

1. INTRODUCTION

Coalbed methane (CBM) is a clean energy source,[1,2] so the mining technology of CBM has gradually attracted attention, but the low permeability of the reservoir significantly limits CBM extraction. The hydraulic permeability enhancement technology method is the most commonly used, but the water pollution and the impact of water lock reaction on subsequent mining are difficult to be solved effectively. Based on this, the use of liquid nitrogen (LN2) for permeation can effectively avoid these disadvantages of hydraulic permeation enhancement, and the research and engineering application prospects of LN2 permeation enhancement technology are also more promising.[3,4]

When LN2 contacts coal rocks, it promotes the generation and development of coal rock pores through temperature stress, freezing, and swelling forces and changes the mechanical properties of coal rocks. In order to clarify the law of LN2 promoting the development of pore structure in coal rock, related scholars have conducted a lot of research studies. Cha et al.[5] demonstrated that LN2 can cause fractures inside the rock, forming a large number of microfractures and destroying the rock structure. Zhang et al.[6] used a low-pressure LN2 jet to impact granite specimens. The results show that LN2 jet can significantly improve rock permeability, and the number of cracks is directly proportional to the temperature of the rock itself. Cai et al.[7] studied the effect of LN2 on rock permeability by comparing rock pore structure before and after LN2 treatment. The results show that LN2 as a fracturing fluid will increase the reservoir volume during fracturing. Li et al.[8] conducted a nuclear magnetic resonance (NMR) test on coal and rock samples after LN2 freeze–thawing treatment and found that coal and rock samples' porosity increased significantly after freeze–thawing. The increasing effect increased with the water saturation of coal and rock samples. Wei et al.[9] conducted LN2 freeze–thaw cycle experiments on coal samples with different water saturations. The results show that the different degrees of internal and external damage of coals with different water saturation are mainly due to the

Received: November 8, 2021
Accepted: January 21, 2022
Published: February 2, 2022

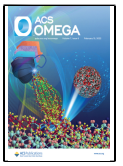

https://doi.org/10.1021/acsomega.1c06296
ACS Omega 2022, 7, 5206–5216

phase change and pore water migration. Qin et al.[10] conducted an NMR test on freeze−thawed coal samples and found that the pore diameter in coal tends to increase with the freezing time. Coetzee et al.[11] found that the use of LN2 as a fracturing fluid could effectively promote the development of internal fractures and increase the permeability of the coal. Scholars examined the LN2 freeze−thawed coal rocks by various technical means and analyzed the effect of liquid nitrogen freeze−thawing on the pore structure of coal rocks. Some scholars also found that this effect decreases with the increase in the number of LN2 freeze−thaw cycles, but there is no relevant research to explore this decay law in depth.[12] During the freezing of coal rocks by LN2, the mechanical properties change with the development of the pore structure in coal rocks.[13] Al-Omari et al.[14] found that rock water saturation has a great influence on the damaging effect of freeze−thaw cycles. Liu et al.[15] studied the rock mechanical behavior under different temperatures and found that the uniaxial compressive strength and Young's modulus increased with temperature decreased. Cai et al.[16] conducted a comparative test between cold-treated and intact coal. The experimental results show that very low temperatures will increase the initial damage of degree of coal and rock. Sandstr et al.[17] carried out rock freeze−thaw cycle tests showing that the number of freeze−thaw cycles impacts rock mechanical properties and damage cracks. Zhai et al.[18] found that the number of freeze−thaw cycles was an important factor in the formation of larger pores in coal, and the proper control of the number of cycles helped achieve effective fracturing of coal. Henwan et al.[19] conducted a study on the strength of coal bodies under the action of cold loading cycles, and the results showed that cold loading had a significant effect on the development of primary fracture structures in coal samples. The temperature gradient formed when LN2 comes in contact with coal destroys the skeleton of the rock, creating many cracks and changing the mechanical properties of the rock.[20] Most previous studies focused on the effects of low-temperature LN2 on the mechanical properties and physical structural damage of coal rocks and elaborated the fracture development mechanism of LN2 freeze−thaw coal rocks in terms of the changes of mechanical parameters such as compressive strength and elastic modulus and the degree of damage to the physical structure of coal rocks. However, the law of coal weakening and pore structure development caused by the number of LN2 freeze−thaw cycles has not been deeply explored.

Research on the influence of LN2 freeze−thaw cycle times on the development of coal pore structure and mechanical properties mostly focuses on the influence of LN2 freeze−thawing, ignoring that with the increase of cycle times, the adaptability of coal is also enhanced and the transformation effect is reduced. This paper focuses on the evolution law of coal pore structure development and mechanical properties under different LN2 freeze−thawing cycle times. Based on the NMR test and mechanical property test, this paper studies the influence law of cycle times on coal weakening and coal pore structure development and reveals the mechanism of LN2 freeze−thawing cycles to transform coal and rock and improve CBM mining efficiency.

2. TEST PREPARATION AND METHOD

2.1. Sample Preparation. In this test, coal seam II-1 of Zhaogu no. 2 mine in Jiaozuo City, Henan Province was selected, and samples were drilled from the same raw coal sample (Φ 50 mm × 100 mm standard cylindrical coal sample) and polished to make both ends smooth and neat. The prepared samples were grouped and numbered in turn, as shown in Figure 1, and the grouping information of coal samples is shown in Table 1.

Figure 1. Coal sample.

Table 1. Coal Sample Grouping

experimental condition	original coal	LN2 freeze−thaw cycle 5 times	LN2 freeze−thaw cycle 10 times	LN2 freeze−thaw cycle 15 times
mechanical property test	A	B	C	D
NMR test	E_0	E_5	E_{10}	E_{15}

2.2. Experimental System.

(1) This experiment adopts the independently developed LN2 cold immersion device, including the self-pressurized LN2 tank and LN2 insulation tank (Figure 2).

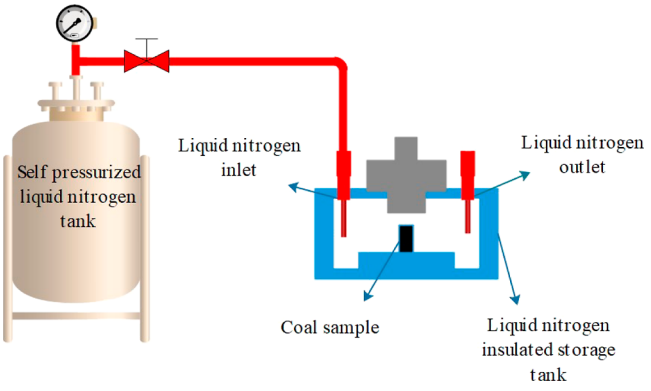

Figure 2. Schematic diagram of LN2 cold immersion device.

(2) NMR test system: The experimental equipment (Figure 3) consists of a MesoMR23-060H-1 low field NMR analyzer from Suzhou Numag Electronic Technology Co., Ltd. Experimental conditions were as follows (Table 2).

(3) Mechanical property test system: A digitally controlled electro-hydraulic servo RMT-150 test machine was used, as shown in Figure 4. The experiment adopts stroke control, and the loading speed is 0.5 mm/s (Table 3).

2.3. Experimental Methods and Process. In this paper, in order to analyze the influence of different numbers of freeze−thaw cycles of LN2 on the change of physical properties and pore structure development of coal, uniaxial

https://doi.org/10.1021/acsomega.1c06296
ACS Omega 2022, 7, 5206−5216

Figure 3. NMR test system.

Table 2. Experimental Parameters of the NMR Test System

NMR test system	main magnetic field strength	resonance frequency	RF pulse frequency	control cabinet magnet temperature
	0.5 T	21.68 MHz	21.68 MHz	32 ± 0.01 °C

Figure 4. Mechanical properties test system.

compression mechanical property tests and NMR tests were conducted on the original coal samples, 5 times freeze−thawed coal samples, 10 times freeze−thawed coal samples, and 15 times freeze−thawed coal samples. The change of mechanical properties of coal samples was analyzed by the results of the mechanical properties test, and the development of pore structure of coal samples was analyzed by the area of transverse relaxation time T_2 spectra of the NMR text. The results of mechanical property tests and NMR tests were combined to find out the effect of pore space structure development on the mechanical properties of coal samples. In order to exclude chance and ensure the reliability of experimental results, all coal samples were drilled from an identical piece of raw coal and parallel experiments were conducted. The LN2 injection device was used to cold leach the coal samples with LN2 in this experiment. The pore distribution and mechanical properties of coal samples were tested by the NMR and mechanical property test systems, respectively. The specific steps were as follows: the coal sample was placed into the vacuum drying oven for drying and weighed intermittently until the coal sample's weight did not change, and the coal sample was regarded as completely dry (drying temperature set to 60 °C). A negative pressure water saturation device was used to saturate the dry coal sample, and then the water was balanced in a constant pressure and constant temperature box (set the vacuum value to −0.1 MPa). Three groups of coal samples, B, C, and D, were subjected to 5, 10, and 15 freeze−thaws with the LN2 injection device. For the purpose of parallel experiments, three coal samples were taken from each group A, B, C, and D, for a total of 12 coal samples. The NMR samples were prepared as follows. The E_0 represents the untreated coal sample, E_5 was obtained after five cycles of E_0 in LN2 freeze−thaw; E_{10} was obtained after five cycles of E_5 in LN2 freeze−thaw; and E_{15} was obtained after five cycles of E_{10} in LN2 freeze−thaw. NMR tests were performed on coal samples E_0, E_5, E_{10}, and E_{15}. The mechanical test system is used to test the mechanical properties of groups A, B, C, and D of coal samples under uniaxial compression. The experimental process is shown in Figure 5, the relevant parameters of the coal samples are shown in Table 4:

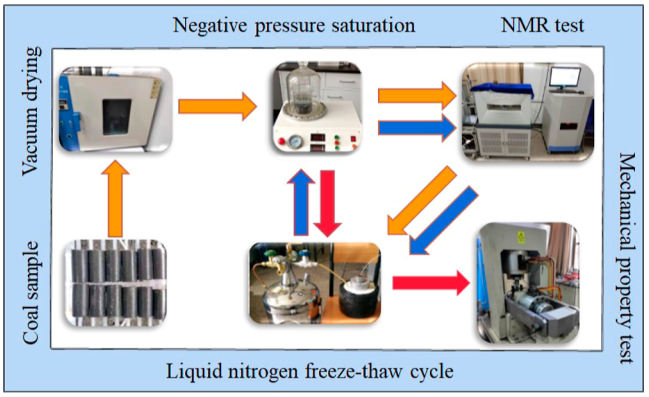

Figure 5. Test flow chart.

2.4. Principles and Theory of NMR. The resonance relaxation between the hydrogen nuclei and the magnetic field in the coal samples was detected by NMR, and then the relaxation characteristics of the hydrogen nuclei in the coal pore structure were investigated. In NMR detection, the distribution characteristics of pore structure and the change law of pore structure can be analyzed according to the transverse relaxation time T_2 spectrum.[21] The relationship between the transverse relaxation time T_2 and the pore diameter r is expressed as formula 1[22]

$$r = T_2 \rho F_s \quad (1)$$

where T_2 is the transverse relaxation time; ρ is the transverse surface relaxation rate; F_s is the shape factor of pore structure; and r is the pore diameter of the coal sample.

Table 3. Experimental Parameters of the Mechanical Property Test System

mechanical property test system	the maximum load	the maximum confining pressure	the deformation rate	the loading rate
	1000 kN	50.0 MPa	0.0001−1.0 mm/s (level 13)	0.01−100.0 kN/s (level 13)

https://doi.org/10.1021/acsomega.1c06296
ACS Omega 2022, 7, 5206−5216

Table 4. Relevant Parameters of the Coal Samples[a]

sample	test	height (mm)	TRD (g·cm^{-3})	ARD (g·cm^{-3})	proximate (wt %)		
					M_{ad}	A_{ad}	V_{daf}
A_1	mechanical property test	100.00	1.51	1.42	0.43	8.12	10.59
A_2		99.90	1.51	1.42	0.43	8.12	10.59
A_3		100.37	1.51	1.42	0.43	8.12	10.59
B_1		100.11	1.51	1.42	0.43	8.12	10.59
B_2		100.20	1.51	1.42	0.43	8.12	10.59
B_3		100.57	1.51	1.42	0.43	8.12	10.59
C_1		100.43	1.51	1.42	0.43	8.12	10.59
C_2		100.61	1.51	1.42	0.43	8.12	10.59
C_3		100.41	1.51	1.42	0.43	8.12	10.59
D_1		100.33	1.51	1.42	0.43	8.12	10.59
D_2		100.21	1.51	1.42	0.43	8.12	10.59
D_3		100.10	1.51	1.42	0.43	8.12	10.59
E	NMR test	100.06	1.51	1.42	0.43	8.12	10.59

[a]A represents original coal samples; B represents coal samples after 5 LN2 freeze−thaw cycles; C represents coal samples after 10 LN2 freeze−thaw cycles; D represents coal samples after 15 LN2 freeze−thaw cycles; E_0, E_5, E_{10}, and E_{15} indicate the stages of coal sample E at different numbers of LN2 freeze−thaws (single LN2 freezing time of coal sample of is 60 min; single thawing time of 4 h for coal samples at 25 °C); TRD represents true density; ARD represents apparent density; M_{ad} represents moisture, air-drying base; A_{ad} represents ash yield, air-drying base; V_{daf} represents volatile matter dry ash-free basis.

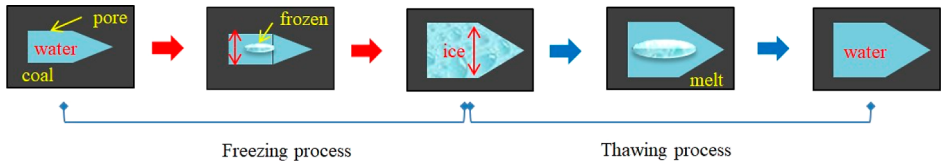

Figure 6. Fracture extension process of water-bearing coal under the LN2 freeze−thaw cycle.

The NMR obtains the spin echo string attenuation curve in the coal pore through the CPMG pulse sequence test and processes the obtained attenuation constant to obtain the transverse relaxation time T_2 distribution, which is non-destructive and highly efficient. In the NMR test, the transverse relaxation time T_2 of a saturated water coal sample is closely related to the pore structure distribution and has a corresponding relaxation time for different phase states of coal.[23,24]

3. DAMAGE MECHANISM OF COAL UNDER FREEZE−THAWING OF LN2

Under the LN2 freeze−thaw cycle conditions, temperature stress and frost heaving force affect the coal, following the volume cycle change law of "freeze shrinkage-frost heave-freeze shrinkage".[25] Studies have shown that the damage degree of coal caused by LN2 freeze−thaw cycles is mainly determined by temperature stress, frost heaving force, and expansion force.[26,27] It is embodied in pore water frost heaving, coal matrix shrinkage, and high-pressure nitrogen expansion. When the coal matrix meets LN2, it shrinks rapidly due to low temperature and changing pore structure. On the other hand, the pore water of coal expands during freezing and transforms the primary fractures, which are continuously developed in the freeze−thaw cycle (Figure 6). The formation and development of cracks are the key factors for the expansion of coal damage. From the mechanical point of view, the coal damage expands when the force on the coal matrix is greater than its tensile strength. The stress of the coal matrix under LN2 freeze−thawing conditions is shown in formula 2. The in situ stress factor was not considered in this experiment, as shown in formula 3

$$\sigma = |\sigma_c + \sigma_{FH} + \sigma_s + \sigma_g| \tag{2}$$

$$\sigma = |\sigma_{FH} + \sigma_s + \sigma_g| \tag{3}$$

where σ is the stress of coal matrix; σ_c is in situ stress; σ_{FH} is frost heaving force; σ_s is matrix shrinkage stress; and σ_g is expansion stress.

The tensile strength of the coal matrix on the weak surface of the coal structure is small, which is more likely to become the direction of crack extension and form fatigue damage. As the damage to the coal matrix gradually accumulates, the strain on the coal becomes more prominent, as evidenced by the development of the pore structure at the microscopic level and changes in the mechanical properties at the macroscopic level. The unit volume strain[28] of the coal matrix can be expressed as formula 4, and the coal volume strain can be expressed as formula 5

$$\varepsilon_{vi} = \varepsilon_{ai} + 2\varepsilon_{ri} \tag{4}$$

$$\varepsilon_v = \int_0^{+\infty} \varepsilon_{ai} + 2\varepsilon_{ri}\, di \tag{5}$$

where ε_{vi} is the unit volumetric strain; ε_{ai} is the unit axial strain; ε_{ri} is the unit circumferential strain; ε_v is the volumetric strain, ε_a is the axial strain; and ε_r is the circumferential strain.

The elastic modulus of coal can be expressed as formula 6. Considering the stress and volumetric strain of the coal matrix per unit volume, the elastic modulus per unit volume of the coal matrix under LN2 freeze−thawing condition is expressed as formula 7

$$E = \frac{\sigma}{\varepsilon} \tag{6}$$

https://doi.org/10.1021/acsomega.1c06296
ACS Omega 2022, 7, 5206−5216

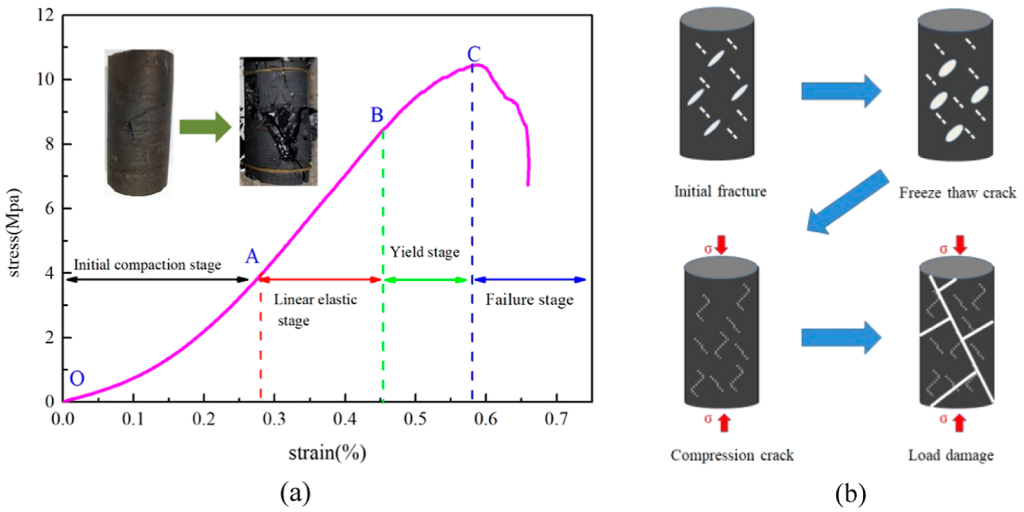

Figure 7. Uniaxial compression test of coal under LN2 freeze−thaw. (a) Stress−strain curve of LN2 freeze−thaw coal. (b) Pore structure change of coal.

$$E_i = |\sigma_{FH} + \sigma_s + \sigma_g|/(\varepsilon_{ai} + 2\varepsilon_{ri}) \quad (7)$$

where: E is the elastic modulus; σ is the stress; ε is the strain; E_i is the elastic modulus per unit volume of coal matrix.

In the mechanical properties test of coal, the elastic modulus can be expressed as formula 8

$$E_d = |\sigma_d|/\varepsilon_a \quad (8)$$

where E_d is the axial elastic modulus of coal. σ_d is the axial stress.

The expressions of the fixed base growth rate and chain growth rate of uniaxial yield limit, T_2 spectrum area, and other parameters are as follows

$$\varphi_a = \frac{S_i - S_0}{S_0} \times 100\% \quad (9)$$

$$\varphi_b = \frac{S_i - S_{i-1}}{S_{i-1}} \times 100\% \quad (10)$$

where φ_a is the fixed base growth rate; φ_b is the fixed specific growth rate, S_i is the second uniaxial yield limit or T_2 spectrum area; and $S_0$is the uniaxial stress yield limit or T_2 spectrum area of coal sample without freeze−thaw cycle.

Under LN2 cold immersion, the frost heaving force σ_{FH}, matrix shrinkage stress σ_s, and the expansion force σ_g are generated through the temperature change, resulting in the increasing stress σ of the coal matrix. When the tensile limit of the coal matrix is exceeded, ε_{vi} begins to accumulate, as shown in formula 4. Under the LN2 freeze−thaw cycle conditions, the coal matrix repeatedly experiences the freeze−thaw process, resulting in many micro deformations ε_{vi} manifested in the change of coal pore structure just as the deformation accumulation in formula 5 corresponds to the increase of T_2 spectrum area. The macroscopic deformation that is difficult to observe directly can be analyzed through the stress−strain change trend of the mechanical properties test reflected in the transformation between formulas 7 and 8. Based on the changes in formulas 9 and 10, the mechanical properties and pore volume changes of coal samples in different freeze−thaw stages and the development law of coal pore structure were analyzed, and the coal damage mechanism under the combination of macro and micro change laws was established.

4. EXPERIMENTAL RESULTS AND DISCUSSION

4.1. Weakening Effect of LN2 Freeze−Thaw Cycle on Coal. *4.1.1. Pore Development Law of Coal Uniaxial Compression Test under LN2 Freeze−Thaw Cycles.* To study the weakening effect of the LN2 freeze−thaw cycle on coal, the stress−strain curve of coal under uniaxial compression was measured. After the LN2 freeze−thawing cycles, the stress−strain curve changes during the uniaxial compression test were measured (Figure 7).

According to the analysis of the experimental results in Figure 7, the cracks of the coal sample are further generated and developed after freeze−thawing with LN2, the total pore volume in the coal increases.[29] When the pore volume of the coal sample is compressed, it leads to coal deformation and damage. Combined with Figure 7a, the stress−strain curve can be divided into four stages: initial compaction, linear elastic, yield, and failure.[30]

The first stage is the initial compaction stage (OA): at this stage, the uniaxial stress compresses the coal's primary and new fracture volume, while causing coal fracture development (OA stage in Figure 7). Pores in coal are the primary bearers of uniaxial stress in the OA stage: only a small part of the uniaxial stress effect on the coal is used for fracture generation and development, and most of it is used for pore collapse to reduce the pore volume in coal. When the uniaxial stress reaches a certain level, the pore volume collapse of the coal reaches its limit, the rate of pore compression of the coal and the increase of the uniaxial stress is unbalanced, and the uniaxial stress will no longer be used mainly for pore volume compression of the coal, leading to the end of the OA stage. Compared with the original coal sample, the LN2 freeze−thawed coal sample promotes the formation and development of pores, delays the arrival of this collapse limit, and increases the OA stage. Figure 7a shows that as the stress increases, the strain in the OA stage increases, but the strain rate decreases. That is, the ability to resist uniaxial stress will be enhanced to some extent as the coal pores are compressed.

The second stage is the linear elastic stage (AB). The AB stage is reached when the pore compression rate and the uniaxial stress increase rate in the coal are unbalanced. The uniaxial stress mainly acts on the elastic deformation of the coal, and the stress−strain curve changes almost linearly in this

https://doi.org/10.1021/acsomega.1c06296
ACS Omega 2022, 7, 5206−5216

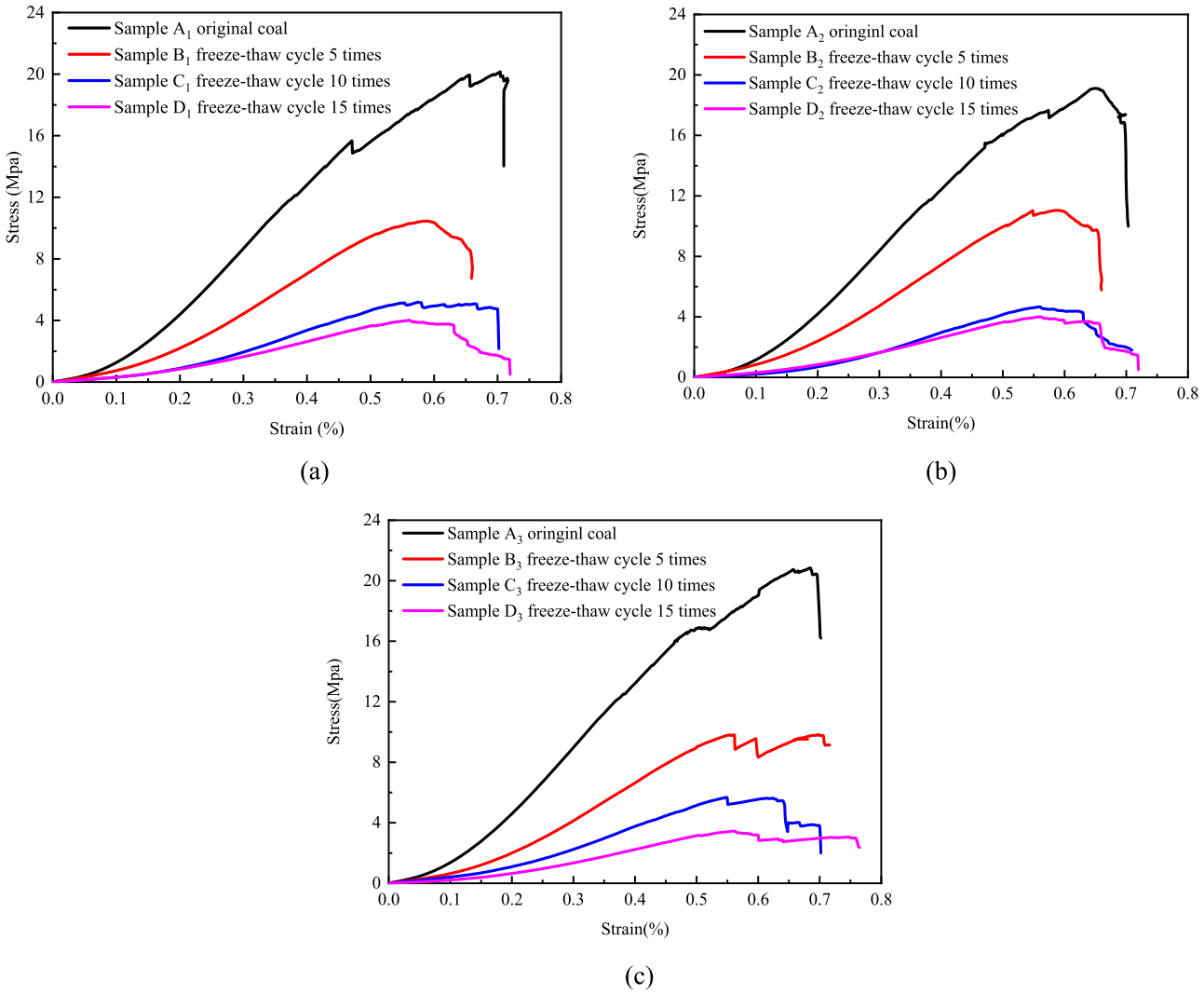

Figure 8. Uniaxial compression test of LN2 freeze−thaw circulating coal. (a) Test group 1. (b) Test group 2. (c) Test group 3.

stage. The AB stage is the transition stage from coal pore closure to coal yield. There is no significant damage to the coal, which is mainly due to the elastic deformation of the coal to withstand the increase in uniaxial stress.

The third stage is the yield stage (BC): At this stage, starting from point B, the balance between the uniaxial stress increase and strain rates is lost again, and many cracks are generated and developed in the coal, resulting in irreversible deformation. The pore structure of coal changes rapidly, and the continuous generation and development of fractures directly lead to penetration of small fractures into large fractures in the coal, which finally leads to the CD stage. With the change of pore structure in the coal, the strain rate increases with uniaxial stress (Figure 7a). There may be two reasons for this result: on the one hand, it is due to the increase of pore volume; on the other hand, it is due to the continuous formation and interconnection of large-scale fractures.

The fourth stage is the failure stage (CD). At this stage, the yield strength of coal reaches the limit, and macro fractures begin to appear. After point C, the strain rate and uniaxial stress of the coal decreased significantly, indicating that the coal began to fracture along the large internal cracks and other positions, shown as coal fracture macroscopically (Figure 7a).

4.1.2. Evolution Law of Stress−Strain Curve of Coal with Different Freeze−Thaw Cycles of LN2. Next, the weakening effect of LN2 freeze−thawing cycles on the mechanical properties of coal was analyzed. Uniaxial compression experiments were carried out on each coal sample after 0, 5, 10, and 15 LN2 freeze−thaw cycles.

The uniaxial compressive stress−strain curves of coal samples in Figure 8a−c comply with the evolution law of Figure 7 and can be divided into initial compaction, linear elastic, yield, and failure stages for analysis. Under the LN2 freeze−thaw cycle conditions, the stress−strain curve of coal will lengthen in the compaction stage and slightly shorten in the elastic and yield stages compared with that of the raw coal, mainly because the LN2 freeze−thaw cycle promotes the development of pore structure and greatly improves the porosity of coal.

According to Figure 8, the uniaxial stress yield limits of coal samples after 0, 5, 10, and 15 LN2 freeze−thaw cycles are in the range of 20 ± 0.7, 10.7 ± 0.4, 5.1 ± 0.5, and 3.7 ± 0.3 MPa, respectively. The uniaxial stress yield limit of coal samples is decreased by 46.5, 74.5, and 81.5% after 5, 10, and 15 cycles, respectively, indicating that the LN2 freeze−thaw cycles greatly reduce the strength of coal. The uniaxial stress yield limit of groups A, B, C, and D coal samples is shown in

https://doi.org/10.1021/acsomega.1c06296
ACS Omega 2022, 7, 5206−5216

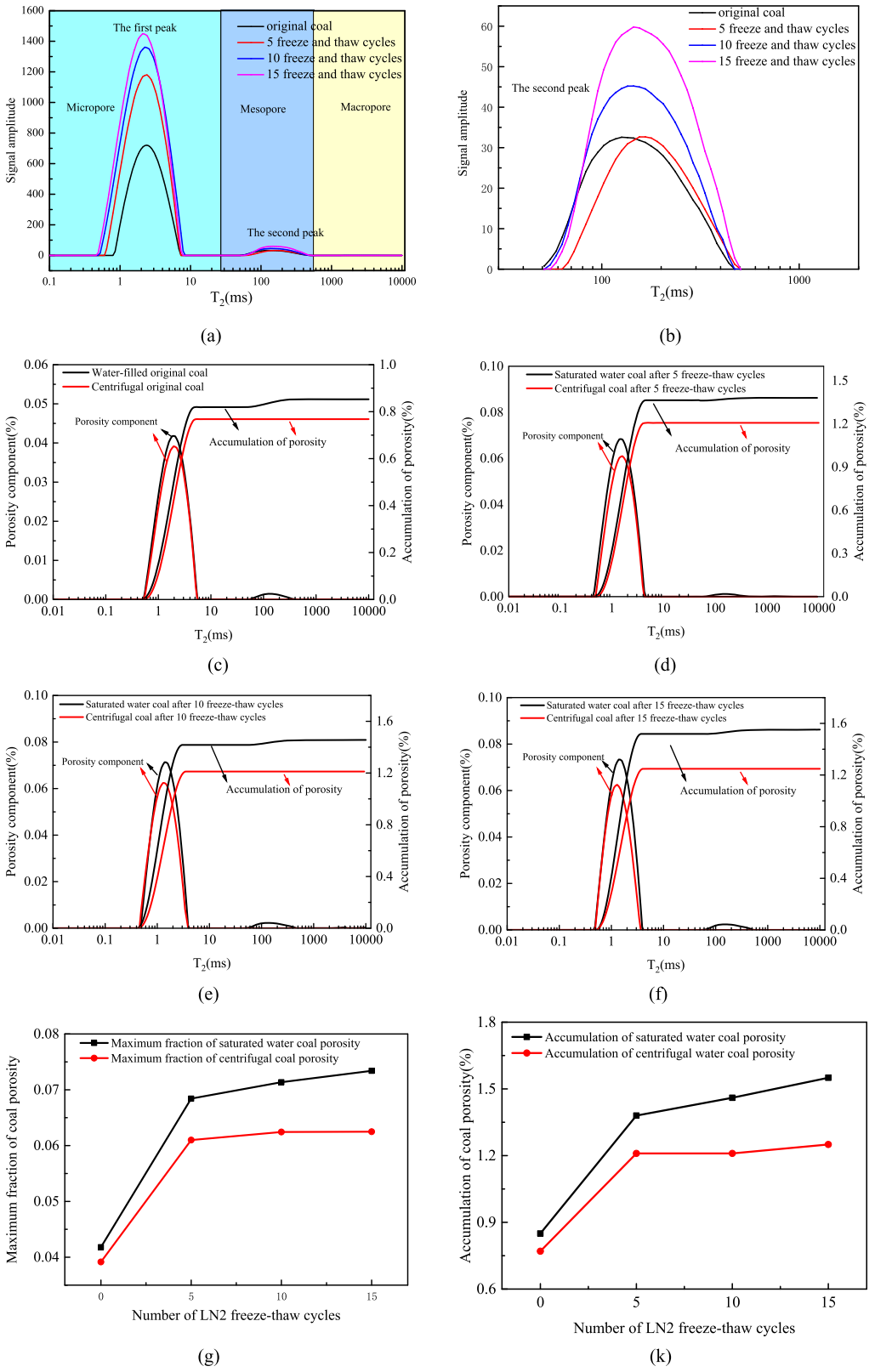

Figure 9. T_2 distribution, porosity for different number of freeze−thaw cycles of LN2. (a) Overall T_2 distribution. (b) Second peak T_2 distribution. (c) Porosity of original coal *n*. (d) Coal porosity after 5 freeze−thaw cycles. (e) Coal porosity after 10 freeze−thaw cycles. (f) Coal porosity after 15 freeze−thaw cycles. (g) Maximum fraction of porosity for different numbers of LN2 freeze−thaw cycles. (k) Accumulation of porosity with different numbers of LN2 freeze−thaw cycles.

Figure 8. Compared with group A, group B decreased by 46.5%; Compared with group B, the uniaxial stress yield limit group C decreased by 50.3%. Compared with group C, the uniaxial stress yield limit of group D decreased by 27.5%. The analysis shows that the decreased range of uniaxial stress yield limit of coal is unchanged after 0−10 LN2 freeze−thaw cycles.

https://doi.org/10.1021/acsomega.1c06296
ACS Omega 2022, 7, 5206−5216

After 11−15 freeze−thaw cycles, the uniaxial stress yield limit is reduced by 45.3%, indicating that the coal sample has certain adaptability to the LN2 freeze−thaw process, and the coal sample transformation is greatly affected reduced. The experimental results of mechanical properties show that the effect of the LN2 freeze−thaw cycle on reducing the strength and elastic modulus of coal is remarkable. After intermittent thawing for 10 cycles (10 h), the reduction of uniaxial stress yield limit and elastic modulus of coal samples did not change significantly. After 11−15 LN2 freeze−thaw cycles, the reduction of uniaxial stress yield limit and elastic modulus of coal samples began to decrease. The reduction efficiency of the LN2 freeze−thaw cycle for coal sample strength and elastic modulus decreased significantly in this process.

4.2. Effect of Freeze−Thaw Cycles of LN2 on the Development of Coal Pore Structure. To better study the influence of the number of LN2 freeze−thaw cycles on the development of coal pore structure and analyze the relationship between the change of coal pore structure and the change of coal mechanical properties, NMR was used to examine coal sample E. The NMR detection results are shown in Figure 9.

Because the experimental coal sample is anthracite, the transverse relaxation rate ρ of coal samples is 1.6 μm/s; combined with formula 1, it is known that T_2 has a positive correlation function with pore diameter, so pores in different pore diameter ranges are divided according to T_2.[31] In Figure 9a, the first wave peak corresponds to micropores, and the pore diameter is less than 0.1 μm. The corresponding aperture of the second wave peak is 0.1−1 μm range. According to the test results, the coal pore size is divided into three areas, in which the micropores belong to adsorption pores, and the medium and large pores belong to seepage pores.[32] In Figure 9a, the peak value of the first wave is much higher than that of the second wave, indicating that the microporous fractures of the coal sample are well developed. After the LN2 freeze−thaw cycle, the peak value of the first wave rises considerably, and the peak value of the second wave also shows an upward trend, indicating that the LN2 freeze−thaw cycle promotes the development of coal fractures, especially micropores. After 5, 10, and 15 cycles of freeze−thawing with LN2, the full pore T_2 spectral area increased by 4911, 29,981, and 38,261, respectively, and the fixed base growth rates were 44.1, 269.0, and 343.3%, respectively. The T_2 spectral areas of adsorption holes increased by 1703, 3025, and 3282, respectively, and the growth rates of the fixed base were 71.5, 127.0, and 137.8%, respectively. The T_2 spectral area of the seepage hole increased by 3208, 26,956, and 34,879, and the fixed base growth rates were 36.6, 307.6, and 396.0%, respectively. LN2 freeze−thawing cycle 10 times more than 5 times T_2 spectrum area full hole increased by 25,070 with a chain growth rate of 156.2%, the adsorption holes increased by 1322 with a chain growth rate of 32.4%, and the seepage hole increased by 23,748 with a chain growth rate of 198.4%. The LN2 freeze−thawing cycle 15 times more than 5 times T_2 spectrum area full hole increased by 8280 with a chain growth rate of 20.1%, the adsorption holes increased by 257 with a chain growth rate of 4.8%, and the seepage hole increased by 7923 with a chain growth rate of 22.2%. The porosity components and accumulated porosity of coal samples before and after centrifugation with different numbers of freeze−thaw cycles of LN2 are shown in Figure 9c−f, and the porosity changes can be clearly observed in combination with Figure 9g,k. The growth curves of Figure 9g,k all gradually leveled off during the process of maximum porosity fraction from 0.0418 to 0.07339% and cumulative porosity from 0.85274 to 1.55196% for the water-saturated coal sample. Similarly, the maximum fraction of porosity and cumulative porosity growth curves of centrifugal coal samples gradually leveled off. The experimental results showed that the maximum porosity fraction and cumulative porosity of coal sample decreased substantially in the increment of 6−10 freeze−thaw stages, and basically did not increase during 11−15 freeze−thaw stages. The maximum porosity fraction and cumulative porosity of the centrifugal coal sample did not increase significantly during the 6−15 freeze−thaw stages.

Figure 9 shows that after the LN2 freeze−thawing cycle, the T_2 spectral area of the coal increases and the number of full pores, adsorption pores, and seepage pores gradually increases.[33] By comparing the chain growth rate of T_2 spectral area of the full, seepage, and adsorption holes in the 5, 10, and 15 freeze−thawing cycles, the chain growth rate of T_2 spectral area of adsorption hole in the 0−5th freeze−thawing cycles is larger than that in the 6−10 freeze−thawing cycles. The chain growth rate of the T_2 spectral area of adsorption pore and seepage pore decreased significantly during the 11−15 stages. Table 5 shows the comparison of the chain growth rate of the

Table 5. T_2 Spectrum Specific Growth Rate in the Same Stage

freeze−thaw cycles	full hole (%)	adsorption pore (%)	seepage hole (%)
0−5	44.1	71.5	36.6
6−10	156.2	32.4	198.4
11−15	20.1	4.8	22.2

T_2 spectral area of different times of LN2 freeze−thawing cycles. With the increase of LN2 freeze−thawing cycles, the adaptability of coal samples to LN2 freeze−thawing cycles is gradually enhanced. The difference in porosity variation between saturated and centrifuged coal samples in Figure 9g,k indicates that the modification is mainly carried out within the pore space where free water is located during the 6−10 freeze−thaw stages. After 5 freeze−thaw cycles, the ability of the adsorption hole to accept the transformation decreased significantly; after 6−10 cycles, the percolation efficiency is the highest, and after 10 freeze−thawing cycles, the efficiency of coal pore structure modification decreases greatly. The transformation effect of the full hole is considerable in 0−10 freeze−thawing cycles, and the transformation efficiency of 11−15 freeze−thawing cycles is greatly reduced. When the number of freeze−thaw cycles increases, the full pores develop gradually, and the trend of increasing the number of seepage pores lags behind the trend of increasing the number of adsorption pores. Combined with the analysis in Table 5, the reason is that the pore development follows the order from small size to large size, and the adsorption pores will continuously develop and penetrate each other during the freeze−thaw cycle of LN2, and then form seepage pores, and finally form frost swelling cracks on the surface of coal.

4.3. Effect of Pore Structure Change on Mechanical Properties of Coal Samples under LN2 Freeze−Thawing Cycles. Coal is a multipore structure, and cracks can be formed and developed after the LN2 freeze−thawing cycle, thus affecting the mechanical properties of the coal. When LN2 contacts coal, temperature stress will be generated and pore water in the pore structure will be frozen. Theoretically, the

https://doi.org/10.1021/acsomega.1c06296
ACS Omega 2022, 7, 5206−5216

water-ice phase transformation can produce frost heaving force up to 200 MPa.[17] Under LN2 freeze−thawing cycle, temperature stress and frost heaving force act on coal pore structure together[34,35] and promote pore development. To better study the influence of the change of coal pore structure on the mechanical properties, the relationship between the base reduction rate of coal uniaxial stress yield limit and the base growth rate of full pore T_2 spectral area was analyzed in combination with the results of mechanical properties and NMR tests. The change rate trend of the fixed base is shown in Figure 10.

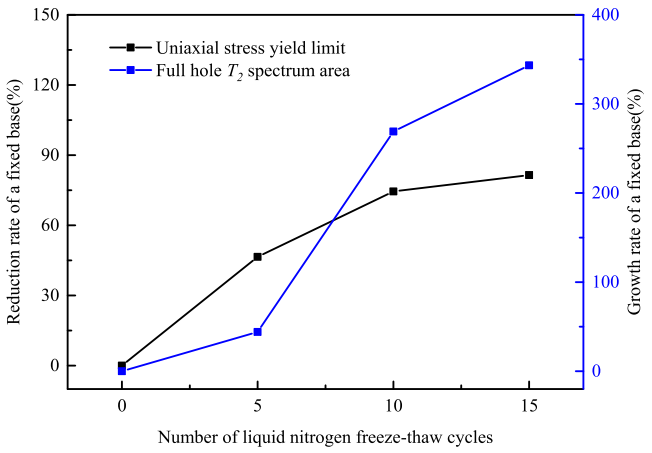

Figure 10. Variation trend of uniaxial stress yield limit and T_2 spectral area.

According to the analysis of Figure 10, the uniaxial stress yield limit of the coal sample is inversely proportional to the full hole T_2 spectral area, and the base reduction rate of the uniaxial stress yield limit and the base growth rate of full hole T_2 spectral area are increasing. In the 0−5 LN2 freeze−thaw cycles, the increase of the T_2 spectrum area of the adsorption hole is the most prominent, and the uniaxial stress yield limit of a coal sample is significantly reduced. In the stage of 6−10 LN2 freeze−thaw cycles, the growth rate of T_2 spectral area of adsorption hole decreases, the growth rate of T_2 spectral area of seepage hole increases significantly, and the growth rate of T_2 spectral area of full hole increases, but the decline rate of uniaxial stress yield limit decreases. In the stage of 11−15 LN2 freeze−thaw cycles, although the T_2 spectrum area of coal samples is still rising, the growth rate is significantly lower than that in the previous stage, and the reduction trend of uniaxial stress yield limit also tends to be gentle, which can be regarded as the significant reduction of coal sample efficiency in LN2 freeze−thaw transformation at this stage, which is not in line with the actual application benefit. The author believes that under the condition of the LN2 freeze−thaw cycle, the new cracks in the coal sample meet the time evolution order from adsorption holes to seepage holes; that is, the pore diameter gradually increases, and the increase of the number of adsorption holes has a more significant impact on the uniaxial stress yield limit of the coal sample. In the experimental process, the increased adsorption pore volume can be regarded as increasing new fracture volume. The increase of seepage pore volume mainly depends on the development of adsorption pores and the generation and development of new fractures. Combined with the experimental results of 0−5 times and 6−10 times, it can be seen that the new fracture plays a more significant role in weakening the coal than the original fracture. With the increase of pore volume of the coal sample, the uniaxial stress yield limit and elastic modulus generally decrease, especially in 0−5 experiments. The increase of adsorption pore volume has a greater impact on the mechanical properties of coal.

5. CONCLUSIONS

In this paper, the pore structure development and mechanical parameters of coal samples with different LN2 freeze−thaw cycles were characterized by uniaxial stress yield limit, elastic modulus, and T_2 spectrum area. Based on this, the coal development mechanism under different LN2 freeze−thaw cycles is revealed from the parameter changes of coal mechanical properties and pore structure development. The following conclusions were drawn.

(1) Under the LN2 freeze−thaw cycle condition, the initial compaction stage of the coal stress−strain curve becomes longer, and the elastic stage and yield stage become shorter, indicating that the pore volume of coal has increased, the structure has been damaged, and its strength has been reduced. The LN2 freeze−thaw cycle will weaken the coal, promote the development of coal pore structure, and then improve the exploitation efficiency of CBM.

(2) LN2 freeze−thaw cycle will greatly reduce the uniaxial stress yield limit and elastic modulus of coal: in the stage of 0−10 freeze−thaw cycles, the reduction range does not change, the transformation capacity decreases in the stage of 11−15 freeze−thaw cycles, the reduction range of uniaxial stress yield limit decreases by 45.3%, the change of elastic modulus tends to be gentle, and the adaptability of coal samples to LN2 freeze−thaw cycle is enhanced.

(3) Under the LN2 freeze−thaw conditions, the promotion of coal adsorption pore development is most evident in 0−5 cycles, the development effect of coal seepage pore in 6−10 cycles occupies the leading position, and the efficiency of full pore transformation in 11−15 cycles decreases by 87.13%. The change of seepage hole volume shows that the improved efficiency of coal permeability is the highest in the stage of 6−10 LN2 freeze−thaw cycles. According to the changes of pores in different pore sizes, the development of coal pore structure follows the sequence from adsorption pore to seepage pore, that is, from small to large.

(4) By comparing the base reduction rate of uniaxial stress yield limit, the change trend diagram of elastic modulus, and the base growth rate of T_2 spectrum area, it is found that when the number of adsorption holes increases, the uniaxial stress yield limit and elastic modulus of coal decrease more greatly, indicating that the increase of the number of adsorption holes has a greater impact on the uniaxial stress yield limit and elastic modulus of coal. Based on the influence of the increase of the number of adsorption holes and seepage holes on the uniaxial stress yield limit and elastic modulus of coal, it can be seen that under the condition of the same volume growth, the adsorption holes have a more significant influence on the uniaxial stress yield limit and elastic modulus of coal than the seepage holes.

https://doi.org/10.1021/acsomega.1c06296
ACS Omega 2022, 7, 5206−5216

AUTHOR INFORMATION

Corresponding Author

Bo Li − *School of Safety Science and Engineering, Henan Polytechnic University, Jiaozuo 454003, China; Collaborative Innovation Center of Coal Work Safety and Clean High Efficiency Utilization, Henan Polytechnic University, Jiaozuo 454003, China; State Key Laboratory Cultivation Base for Gas Geology and Gas Control, Henan Polytechnic University, Jiaozuo, Henan 454003, China;* orcid.org/0000-0002-6767-2982; Email: anquanlibo@163.com

Authors

Zhen Shi − *School of Safety Science and Engineering, Henan Polytechnic University, Jiaozuo 454003, China*

Zeqi Wang − *School of Safety Science and Engineering, Henan Polytechnic University, Jiaozuo 454003, China*

Laisheng Huang − *School of Safety Science and Engineering, Henan Polytechnic University, Jiaozuo 454003, China*

Complete contact information is available at: https://pubs.acs.org/10.1021/acsomega.1c06296

Notes

The authors declare no competing financial interest.

ACKNOWLEDGMENTS

The authors would like to thank the financial support from the National Natural Science Foundation of China (51874125), the Project of Youth Talent Promotion in Henan Province (2020HYTP020), the Outstanding Youth Fund of Henan Polytechnic University in 2020 (J2020-4), the Young Key Teachers from Henan Polytechnic University (2019XQG-10), the Zhongyuan Talent Program-Zhongyuan Top Talent (ZYYCYU202012155), the Training Plan for Young Backbone Teachers of Colleges and Universities in Henan Province (2021GGJS051), the Post-doctoral Scientific Research Fund of Henan Province (Grant No. 240718), and the Key Specialized Research and Development Breakthrough of Henan Province (212102310597, 222102320086).

REFERENCES

(1) Wu, Y.; Liu, J.; Elsworth, D.; Miao, X.; Mao, X. Development of anisotropic permeability during coalbed methane production. *J. Nat. Gas Sci. Eng.* **2010**, *2*, 197−210.

(2) Cheng, L.; Ge, Z.; Chen, J.; Ding, H.; Zou, L.; Li, K. A sequential approach for integrated coal and gas mining of closely-spaced outburst coal seams: Results from a case study including mine safety improvements and greenhouse gas reductions. *Energies* **2018**, *11*, 3023.

(3) Shi, J. Q.; Durucan, S. Drawdown induced changes in permeability of coalbeds: a new interpretation of the reservoir response to primary recovery. *Transp. Porous Media* **2004**, *56*, 1−16.

(4) Fu, J.; Fu, X.; Hu, X.; Chen, L.; Ou, J. Research into comprehensive gas extraction technology of single coal seams with low permeability in the Jiaozuo coal mining area. *Min. Sci. Technol.* **2011**, *21*, 483−489.

(5) Cha, M.; Yin, X.; Kneafsey, T.; Johanson, B.; Alqahtani, N.; Miskimins, J.; Patterson, T.; Wu, Y.-S. Cryogenic fracturing for reservoir stimulation–Laboratory studies. *J. Pet. Sci. Eng.* **2014**, *124*, 436−450.

(6) Zhang, S.; Huang, Z.; Zhang, H.; Guo, Z.; Wu, X.; Wang, T.; Zhang, C.; Xiong, C. Experimental study of thermal-crack characteristics on hot dry rock impacted by liquid nitrogen jet. *Geothermics* **2018**, *76*, 253−260.

(7) Cai, C.; Li, G.; Huang, Z.; Shen, Z.; Tian, S.; Wei, J. Experimental study of the effect of liquid nitrogen cooling on rock pore structure. *J. Nat. Gas Sci. Eng.* **2014**, *21*, 507−517.

(8) Li, B.; Zhang, L.; Wei, J.; Ren, Y. Pore damage properties and permeability change of coal caused by freeze-thaw action of liquid nitrogen. *Adv. Civ. Eng.* **2018**, *2018*, 5076391.

(9) Wei, J.; Zhang, L.; Li, B.; Wen, Z. Non-uniformity of coal damage caused by liquid nitrogen freeze-thaw. *J. Nat. Gas Sci. Eng.* **2019**, *69*, 102946.

(10) Qin, L.; Zhai, C.; Liu, S.; Xu, J.; Yu, G.; Sun, Y. Changes in the petrophysical properties of coal subjected to liquid nitrogen freeze-thaw–a nuclear magnetic resonance investigation. *Fuel* **2017**, *194*, 102−114.

(11) Coetzee, S.; Neomagus, H. W. J. P.; Bunt, J. R.; Strydom, C. A.; Schobert, H. H. The transient swelling behaviour of large (−20 + 16 mm) South African coal particles during low-temperature devolatilisation. *Fuel* **2014**, *136*, 79−88.

(12) Qin, L.; Zhai, C.; Liu, S.; Xu, J. Factors controlling the mechanical properties degradation and permeability of coal subjected to liquid nitrogen freeze-thaw. *Sci. Rep.* **2017**, *7*, 3675.

(13) Li, B.; Zhang, J.; Ding, Z.; Wang, B.; Li, P. A dynamic evolution model of coal permeability during enhanced coalbed methane recovery by N2 injection: experimental observations and numerical simulation. *RSC Adv.* **2021**, *11*, 17249−17258.

(14) Al-Omari, A.; Beck, K.; Brunetaud, X.; Török, Á.; Al-Mukhtar, M. Critical degree of saturation: A control factor of freeze-thaw damage of porous limestones at Castle of Chambord, France. *Eng. Geol.* **2015**, *185*, 71−80.

(15) Liu, Q. S.; Xu, G. M.; Hu, Y. H.; Chang, X. Study on Basic Mechanical Behaviors of Rocks at Low Temperatures. *Trans. Tech. Publ.* **2006**, *306−308*, 1479−1484.

(16) Cai, C.; Gao, F.; Li, G.; Huang, Z.; Hou, P. Evaluation of coal damage and cracking characteristics due to liquid nitrogen cooling on the basis of the energy evolution laws. *J. Nat. Gas Sci. Eng.* **2016**, *29*, 30−36.

(17) Sandstr, O. M. T.; Fridh, K.; Emborg, M.; Hassanzadeh, M. The influence of temperature on water absorption in concrete during freezing. *Nord. Concr. Res.* **2012**, *45*, 45−58.

(18) Zhai, C.; Qin, L.; Liu, S.; Xu, J.; Tang, Z.; Wu, S. Pore structure in coal: pore evolution after cryogenic freezing with cyclic liquid nitrogen injection and its implication on coalbed methane extraction. *Energy Fuels* **2016**, *30*, 6009−6020.

(19) Hewan, L.; WangLaigui, Z.; et al. Study on characteristic of coal sample strength under cyclic cold loading. *J. Saf. Sci. Technol.* **2016**, *12*, 10−14.

(20) Qin, L.; Zhai, C.; Liu, S.; Xu, J. Mechanical behavior and fracture spatial propagation of coal injected with liquid nitrogen under triaxial stress applied for coalbed methane recovery. *Eng. Geol.* **2018**, *233*, 1−10.

(21) Yao, Y.; Liu, D.; Che, Y.; Tang, D.; Tang, S.; Huang, W. Petrophysical characterization of coals by low-field nuclear magnetic resonance (NMR). *Fuel* **2010**, *89*, 1371−1380.

(22) Qin, L.; Zhai, C.; Xu, J.; Liu, S.; Zhong, C.; Yu, G. Evolution of the pore structure in coal subjected to freeze- thaw using liquid nitrogen to enhance coalbed methane extraction. *J. Pet. Sci. Eng.* **2019**, *175*, 129−139.

(23) Cai, Y.; Liu, D.; Pan, Z.; Yao, Y.; Li, J.; Qiu, Y. Petrophysical characterization of Chinese coal cores with heat treatment by nuclear magnetic resonance. *Fuel* **2013**, *108*, 292−302.

(24) Yao, Y.; Liu, D.; Liu, J.; Xie, S. Assessing the water migration and permeability of large intact bituminous and anthracite coals using NMR relaxation spectrometry. *Transp. Porous Media* **2015**, *107*, 527−542.

(25) Matsuoka, N. Mechanisms of rock breakdown by frost action: an experimental approach. *Cold Reg. Sci. Technol.* **1990**, *17*, 253−270.

(26) Kim, K. M.; Kemeny, J. *Effect of Thermal Shock and Rapid Unloading on Mechanical Rock Properties*; OnePetro, 2009.

(27) Ge, J.; Jerath, S.; Ghassemi, A.; Ling, K. *Sensitivity Study on the Poroelastic and Thermoelastic Effects on the Stress Reversal nearby an Existing Hydraulic Fracture*; OnePetro, 2018.
(28) Mao, L.; Hao, N.; An, L.; Chiang, F.-p.; Liu, H. 3D mapping of carbon dioxide-induced strain in coal using digital volumetric speckle photography technique and X-ray computer tomography. *Int. J. Coal Geol.* **2015**, *147−148*, 115−125.
(29) Qin, L.; Wang, P.; Li, S.; Lin, H.; Wang, R.; Wang, P.; Ma, C. Gas adsorption capacity changes in coals of different ranks after liquid nitrogen freezing. *Fuel* **2021**, *292*, 120404.
(30) Qin, L.; Ma, C.; Li, S.; Lin, H.; Wang, P.; Long, H.; Yan, D. Mechanical damage mechanism of frozen coal subjected to liquid nitrogen freezing. *Fuel* **2022**, *309*, 122124.
(31) Zheng, S.; Yao, Y.; Liu, D.; Cai, Y.; Liu, Y. Nuclear magnetic resonance surface relaxivity of coals. *Int. J. Coal Geol.* **2019**, *205*, 1−13.
(32) Yao, Y.; Liu, D.; Cai, Y.; Li, J. Advanced characterization of pores and fractures in coals by nuclear magnetic resonance and X-ray computed tomography. *Sci. China: Earth Sci.* **2010**, *53*, 854−862.
(33) Hassan, J. Pore size distribution calculation from 1H NMR signal and N2 adsorption–desorption techniques. *Phys. B* **2012**, *407*, 3797−3801.
(34) Li, B.; Huang, L.; Lv, X.; Ren, Y. Study on temperature variation and pore structure evolution within coal under the effect of liquid nitrogen mass transfer. *ACS Omega* **2021**, *6*, 19685−19694.
(35) Li, B.; Huang, L.; Lv, X.; Ren, Y. Variation features of unfrozen water content of water-saturated coal under low freezing temperature. *Sci. Rep.* **2021**, *11*, 15398.

https://doi.org/10.1021/acsomega.1c06296
ACS Omega 2022, 7, 5206−5216